Magnetic field effects on organic electrophosphorescence

J. Kalinowski
Department of Molecular Physics, Technical University of Gdańsk, ul. G. Narutowicza 11/12, 80-952 Gdańsk, Poland

M. Cocchi, D. Virgili, V. Fattori, and P. Di Marco
Institute of Organic Synthesis and Photoreactivity, National Research Council of Italy, via P. Gobetti 101, 40129 Bologna, Italy
(Received 16 September 2003; revised manuscript received 5 May 2004; published 3 November 2004)

The electrophosphorescence (EPH) efficiency was found to increase by up to 6% for the devices based on a metallo-organic phosphor of iridium and 2% for those based on a metal-organic complex of platinum as an external magnetic field increased to 500 mT. Also, a difference in the field dependence of the EPH for these devices has been observed. We demonstrate that these experimental findings can principally be understood in terms of the Zeeman and hyperfine interactions of electrons located on phosphor molecules and holes located on the hole-transporting molecules, forming correlated electron-hole pairs in the emitting layer. The difference in the field behavior of the effect for the two phosphors results from their different molecular structures.

DOI: 10.1103/PhysRevB.70.205303 PACS number(s): 78.60.Fi, 78.66.Qn, 73.61.Ph, 85.60.Jb

I. INTRODUCTION

Organic electrophosphorescence (EPH) has become of great interest due to the high quantum efficiency of organic electroluminescent devices based on metallo-organic phosphors as emitters.[1–3] Electroluminescence (EL) (including EPH) is the result of the electric-field imposed formation of emissive states without recourse of any intermediate energy forms, such as heat. If the emissive states are formed in organic matter, the following optical emission is called organic EL. Different types of organic EL can be distinguished depending on the excitation mode of emitting states.[4] Their formation in the recombination process of electrode injected electrons and holes is perhaps the most common mechanism of organic EL. The recombination process and relaxation pathways of elementary excitations are, therefore, of both theoretical and practical importance. Among factors responsible for the EL quantum efficiency is the ratio with which singlet and triplet emissive states are created in the recombination process. In hydrocarbon materials usually only singlet states luminesce, whereas triplet states are usually nonemissive at room temperature.[5,6] An assumption often employed is that excitons are formed in the ratio of one singlet to three triplets, since only a singlet combination $(\uparrow\downarrow\text{-}\downarrow\uparrow)$ can be formed from the addition of two spin $-1/2(\uparrow$ or $\downarrow)$ charge carriers; the triplet states, $(\downarrow\uparrow+\uparrow\downarrow)$, $(\uparrow\uparrow)$, $(\downarrow\downarrow)$, are threefold degenerated in the absence of spin perturbations. As a consequence, the intrinsic EL quantum efficiency of any electrofluorescent diode would be limited to 25%. This purely spin statistics-based prediction of the singlet-to-triplet concentration ratio (1:3) may be subject to a drastic reduction[4,5] or a remarkable increase[7,8] because of carrier energetics and spin-dependent exciton formation cross sections, respectively. While the first one leads to low electrofluorescence efficiencies, the second may increase the electrofluorescence efficiency up to about 42% as found in conjugated polymer-based electrofluorescent diodes.[9,10]

A natural complement or an alternative for enhancing the singlet yield has been the use of phosphorescent species having significant spin-orbit coupling to promote the spin flip needed for optical emission. The most prominent schemes for harvesting triplet excitons led to nearly 90% of the internal EPH efficiency from organic EL diodes based on the highly phosphorescent molecule of an organometallic complex of iridium.[2] However, this impressive result has been attainable only in the low-current regime of the EPH devices that is within a lower limit of their overall light output. A strong roll-off in efficiency at large current densities (high applied fields) is observed with EPH devices as a rule.[1–3,11] This decrease ascribed primarily to triplet-triplet annihilation[11] has been recently shown to be largely affected by electric field-assisted dissociation of electron-hole pairs formed in the recombination process prior to the final emitting states.[3] The estimated intercarrier distance (r) of the separated (but still Coulombically correlated) charge pairs (CPs) ranges from 0.7 to over 3.5 nm, depending on the materials and theoretical models used.[3,12] It determines the ability of a molecular (M) ion pair $(M^+\cdots M^-)$ to form an emissive molecular excited state (M*), excimer (M*M), or a short-distant $(M^+\text{-}M^-)$ pair that can relax radiatively in a sort of cross transition (electromers[12–14]) producing additional emission bands in single-component organic light-emitting diodes (LEDs). Molecularly excited electron donor (D*) and electron acceptor (A*) states, exciplexes $(c_1|A^*D\rangle + c_2|A^-D^+\rangle)$ comprised of locally excited $c_1|A^*D\rangle$ and charge-transfer $c_2|A^-D^+\rangle$ configuration components, and electroplexes $(A^-\text{-}D^+)$[15,16] are corresponding excited states in electron donor (D)–electron acceptor (A) systems, where $(A^-\cdots D^+)$ CPs can be created. The formation processes of all these states have been found to be perturbed by an external electric field,[13,14,16] and they are expected to be magnetic field sensitive, supplying information about the spin evolution of the charge pair states and the spin issue of their final emissive products.

In the present study, we are concerned with the EL efficiency of green and red organic phosphor-doped blends of a diamine derivative (TPD) and polycarbonate (PC) in an external magnetic field (B) to observe possible magnetic field

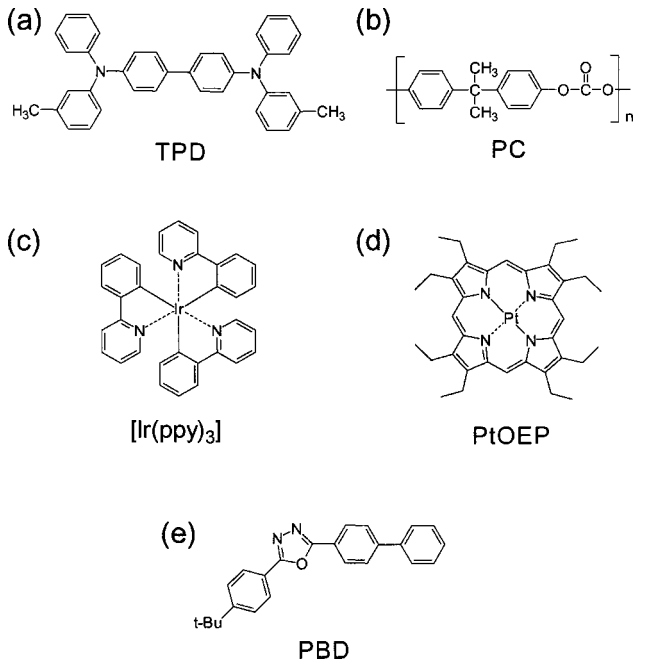

FIG. 1. The molecular structures of materials used in the fabrication of the LEDs studied: (a) TPD (*N*,*N*′-diphenyl-*N*,*N*′-bis(3-methylphenyl)-[1,1′-biphenyl]-4,4′-diamine; (b) PC bisphenol-A-polycarbonate; (c) $Ir(ppy)_3$ *fac* tris(2-phenylpyridine)iridium; (d) PtOEP 2,3,7,8,12,13,17,18-octaethyl-21*H*, 23*H*-porphine platinium (II); and (e) PBD 2-(biphenyl-4-yl)-5-(4-tert-butylphenyl)-1,3,4-oxadiazole.

effects on organic EPH and examine their mechanisms, as they can facilitate the understanding of the formation and decay of emissive states in organic EL devices.

II. EXPERIMENT

The EPH efficiency from the LEDs based on metal-organic phosphors of iridium $[Ir(ppy)_3]$ and platinum (PtOEP) has been measured in the absence and in the presence of a varying magnetic field (B). The double-layer LEDs consisted of the phosphor-doped blends of a diamine derivative (TPD) and polycarbonate (PC) as the emitter and hole-transporting layer (HTL), and a 100% evaporated derivative of oxadiazole (PBD) acting as a hole blocker and electron transporting layer (ETL).[3] The light emission has been observed through a transparent indium-tin-oxide (ITO) substrate forming a hole injecting anode to the HTL, whereas the on top evaporated Ca cathode served as an injector of electrons into the ETL. The molecular structures of the materials used are shown in Fig. 1, and emission spectra of the LEDs in Fig. 2. The photoluminescence (PL) of the doped blend layers and EL spectra of the LEDs are identical, except for the EL spectrum of the undoped (75% TPD:25% PC)/100% PBD LED structure as compared with the PL spectrum of a 60 nm-thick (40% TPD:40% PBD:20% PC) film [Fig. 2(a)]. The broad EL spectra of the latter have been ascribed to the combined emission from a number of bimolecular excited states like exciplex and electroplex produced efficiently in the recombination process at the (TPD:PC)/PBD

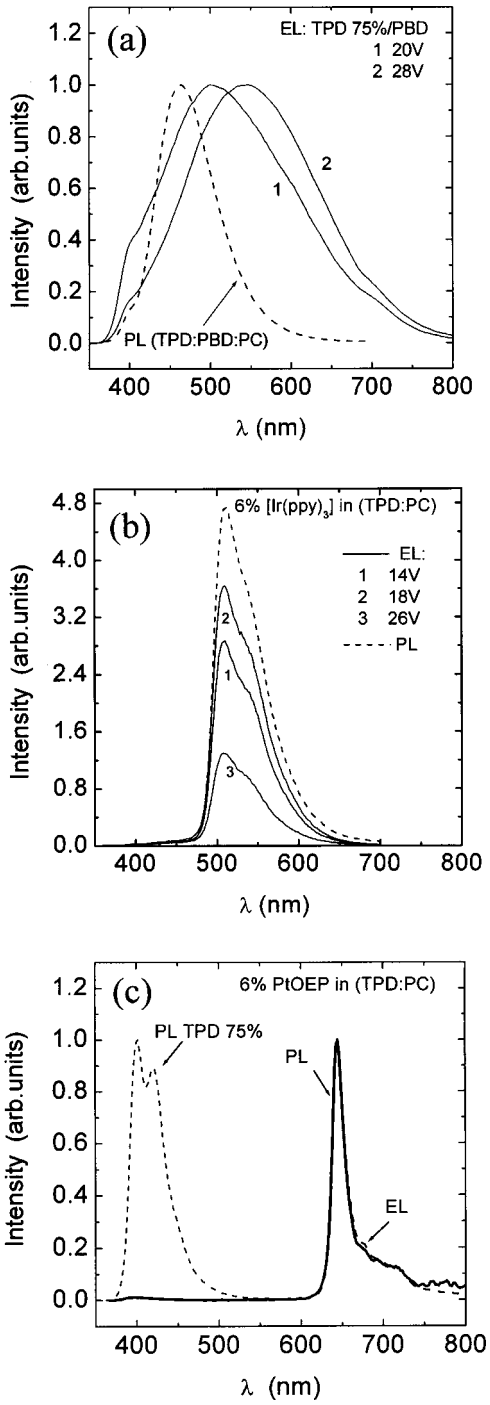

FIG. 2. The photoluminescence (PL) and electroluminescence (EL) spectra of blend films and LED structures fabricated in this work: (a) PL spectrum of a 60 nm thick film of (40 wt% TPD:40 wt% PBD:20 wt% PC), and EL spectra of the ITO/(75 wt% TPD:25 wt% PC) (60 nm)/100% PBD (60 nm)/Ca LED structure, taken at two different voltages (1,2). (b) The PL spectrum of a 50-nm thick [6 wt% $Ir(ppy)_3$:74 wt% TPD:20 wt% PC] film (dashed curve) and its EPH emission in a junction with a 50 nm thick PBD ETL (EL spectra at three different voltages). (c) The EL spectrum of the ITO/(6 wt% PtOEP:74 wt% TPD:20 wt% PC) (60 nm)/100% PBD (60 nm)/Ca device to be compared with its emissive layer and a (75 wt%TPD:25 wt% PC) blend film PL spectra (dashed lines).

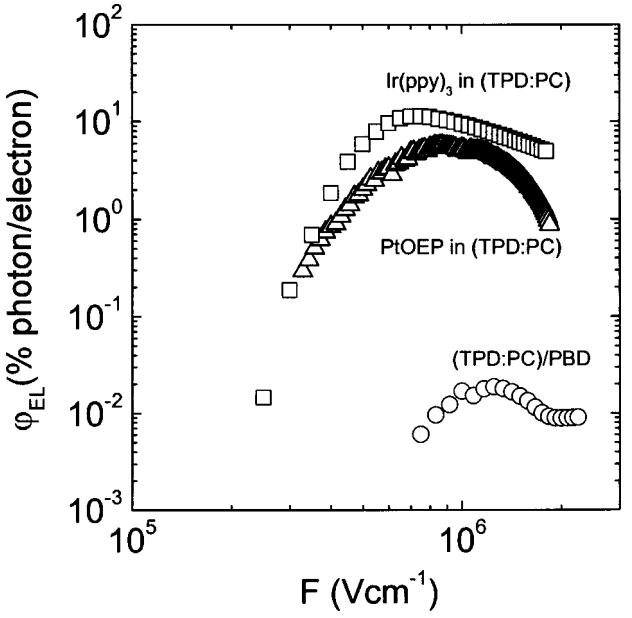

FIG. 3. External quantum efficiency as a function of the applied electric field for three different EL devices described in Fig. 2. The upper point data were obtained with the $Ir(ppy)_3$ (square)- and PtOEP (triangle)-based LED structures, the lower plot with the undoped (TPD:PC) blend HTL.

interface.[16] Clearly, the EL from the phosphor-doped LEDs is due to the radiative decay of excited triplets. Since the quantum efficiency of the bimolecular excited states underlying EL is more than two orders of magnitude lower than that for the phosphor-doped emitter LEDs (Fig. 3), the blend matrix effect on the EPH can be safely neglected. The measured effect of a varying magnetic field on the relative quantum efficiency of all three structures is shown in Fig. 4, and its electric field dependence in Fig. 5. In all cases the magnetic field enhances the emission efficiency, but differences in the maximum effect and functional forms of its B dependence are apparent. No magnetic field effect on the LEDs' driving current was observed.

III. DISCUSSION AND ANALYSIS OF RESULTS

The experimental findings described in Sec. II may be related to various classes and types of the MFE involving triplet states: (I) the first class of phenomena is subject to fine structure modulation (FSM) and requires fields of 10 mT to 0.1 T.[17] This class includes triplet-triplet fusion (T-T) and triplet-charge carrier (doublet species, $D_{\pm 1/2}$) annihilation ($T\text{-}D_{\pm 1/2}$). (II) The second class of phenomena is subject to an electronic Zeeman effect and hyperfine modulation (HFM), and fields of only 1 mT are required.[18] The key examples are photoconduction[19–22] and photochemical reactions[23,24] involving an intermediate charge-transfer state.

The overall second-order rate constants describing class (I) phenomena, specifically the coupling between the triplet-singlet [$\gamma_{TT}^{(S)}$] and triplet-doublet (γ_{Tq}) states, are magnetic field dependent because of the magnetic-field-dependent distribution of a singlet character among the nine ($T\cdots T$) and

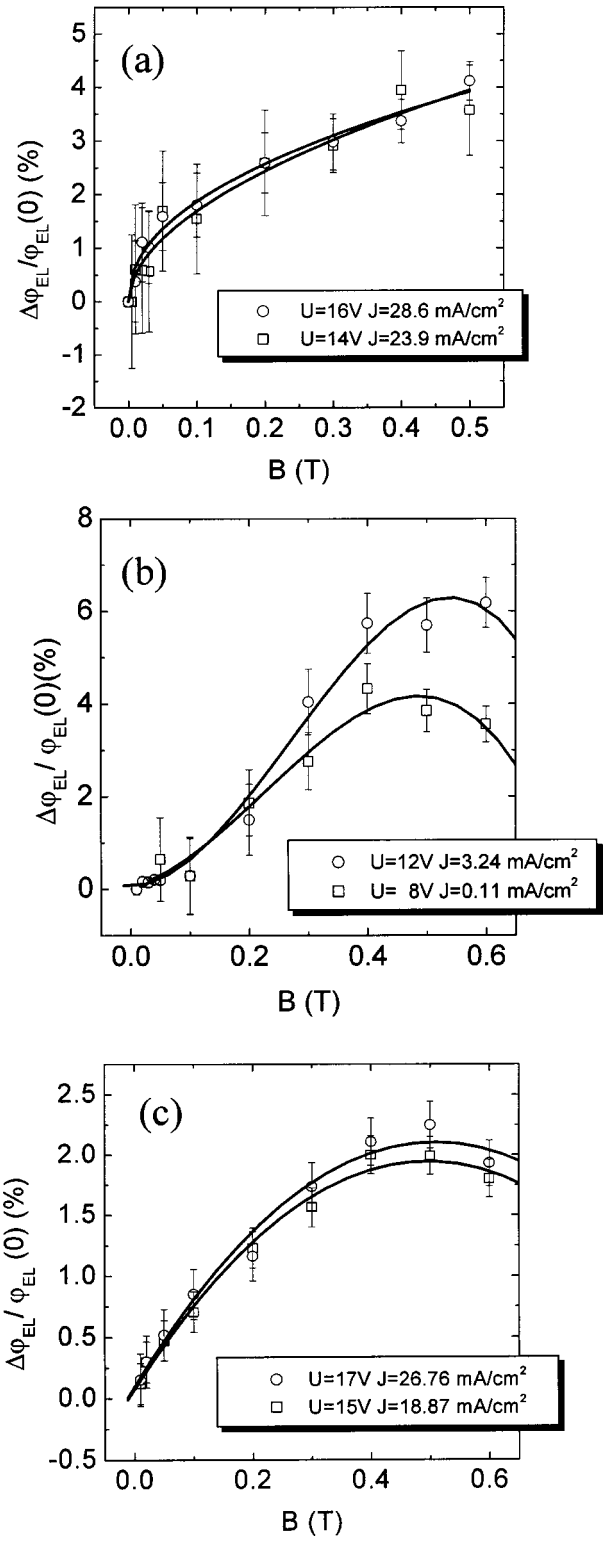

FIG. 4. Observed magnetic field modulation of relative emission efficiency from the LED structures described in Fig. 2: (a) (TPD:PC)/PBD, (b) [$Ir(ppy)_3$:TPD:PC]/PBD, and (c) PtOEP:TPD:PC)/PBD at two different voltages (currents) each.

doublet character among the six ($T\cdots D_{+1/2}$) complex pair states.[25] It has been shown that both $\gamma_{TT}^{(S)}(B)$ and $\gamma_{Tq}(B)$ decrease monotonically at not too high field strengths ($B < 0.2$ T) and saturate at higher fields for random molecu-

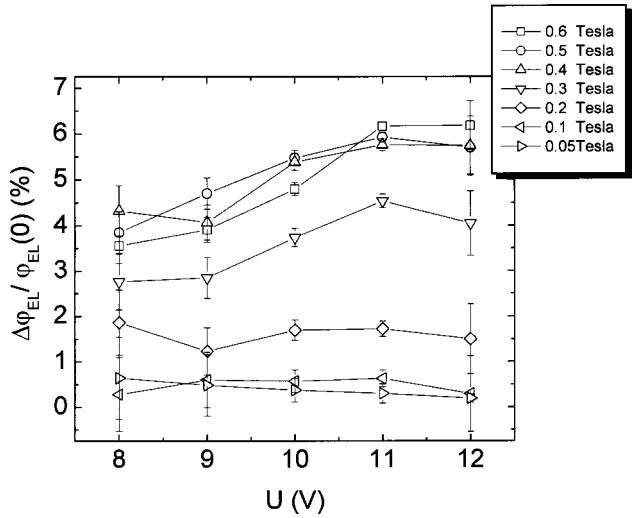

FIG. 5. Plots of the MFEs as a function of applied voltage for the [Ir(ppy)$_3$:TPD:PC]/PBD LED structure, parametric in magnetic field strength (see the inset).

lar systems.[26,27] The field modulation depth is determined by the relation between the Zeeman and the triplet fine-structure parameters, D and E, composing the pair state Hamiltonian.[28] For aromatic molecules, typically D $\cong 10\ \mu$ eV and E/D$\cong$0.1 (cf. Ref. 17), the comparable Zeeman energy is obtained at a magnetic field $\geqslant$100 mT. The zero field splitting in triplet states is similar for trigonal symmetry organometallic complexes like Ir(ppy)$_3$, but differs from that of square planar molecular complexes like porphyrins, where D may exceed 100 μeV,[28] which requires magnetic fields around 1 T in order to get comparable Zeeman energy.

In the phenomena of class (II) external magnetic field controls, the conversion rate between singlet and triplet states of a pair of oppositely charged carriers when the energy separation between their singlet and triplet ground states, $|2J|$, is comparable to or smaller than the difference between the Zeeman energies of the pair components or their hyperfine energies. These effects can be classified into three types:[23,24] (A) the electronic Zeeman effect ($\Delta g\ \beta$B), where $\Delta g = g_e - g_h \neq 0$ is the difference between electron (g_e) and hole (g_h) g factors of the carriers forming pairs; (B) the hyperfine interaction effect; and (C) the mixed effect. Since Δg is usually a small quantity, the first type of effect is not expected to occur at very low magnetic fields and becomes apparent at B$>$1 T.[29] Finally, a combination of the Zeeman ($\Delta g\ \beta$B) and hyperfine interaction (HFI) defines the third type of a mixed effect that will result in a nonmonotonous dependence of the relative yield of the recombination products as the magnetic field strength increases. In this case, an initial low-field increase in the yield becomes followed by its decrease at higher fields and can end with negative values at still higher fields.[24] The maximum occurs at high magnetic fields, e.g., $B_{max}=1-2$ T observed for chain linked phenanthrene and dimethylaniline exciplex fluorescence.[30] The situation becomes more complex if the *e-h* interaction energy (spin-spin and electrostatic exchange) is not negligible. This would be of importance for the short intercarrier distances (r) when $J(r)$ becomes fairly large (larger and/or comparable with $\Delta g\ \beta$B and HFI), and can be considered as class (III) of magnetic field sensitive phenomena. If the degenerate triplet states fall much below the singlet pair state, the splitting of $|T_+\rangle$ and $|T_-\rangle$ spin substates in moderate magnetic field strengths is not sufficient to level $|T_+\rangle$ and $|S\rangle$ states, the hyperfine interaction can be unable to mix these states, no MFE on the recombination products is expected. However, at a level-crossing field, $B_c = |2J|/g\beta$, the hyperfine interaction-induced mixing of these states suddenly sets in, and a sharp change of the product yield follows usually at fields below 100 mT,[31–33] but much higher values of B_c can be observed.[34] As the field increasing proceeds, the $|T_+\rangle$ substate moves above of the $|S\rangle$ level, one would expect a decrease in the mixing rate. The overall MFE signal, if nonzero, is rather weak, showing a nonmonotonous field evolution with an extremum at B_c.

The type of phenomena responsible for the observed MFEs (Fig. 4) depends on the nature of the emissive excited states. Class (I) phenomena cannot be used to interpret the magnetic field-induced emission efficiency change, $[\varphi_{EL}(B) - \varphi_{EL}(0)]/\varphi_{EL}(0) = \Delta\varphi_{EL}(B)/\varphi_{EL}(0)$, for the (TPD:C)/PBD structure [Fig. 4(a)] whose emission is underlain by the bimolecular singlet excited states (TPD^+PBD^- and TPD^+-PBD^-) formed at the organic layers interface.[16] The only possibility that could justify the positive MFE in the framework of the FSM, the singlet fission into two triplets, is ruled out by the small singlet-triplet splitting when two unpaired electrons are localized in the complex components.[35] The FSM could, in principle, explain the experimental observation that an external magnetic field enhances the EL efficiency of the phosphor-doped structures [Figs. 4(b) and 4(c)] whose emission is underlain by the molecular excited triplet states ^{3}Ir(ppy)$_3$* and ^{3}PtOEP*. However, it is difficult to perform a quantitative calculation of the enhancement,[25,26] since there is a number of parameters of an unknown or uncertain value. These are the fine structure splitting parameters D and E, and the rate constants of the $(T\cdots T)$ and $(T\cdots D_{\pm 1/2})$ pair formation (k_1) and backscattering of their component particles from the pair states (k_{-1}). Nevertheless, a qualitative judgment on the applicability of the FSM mechanism can be approached from the general shape of the MFE versus B plots presented in Figs. 4(b) and 4(c), and the voltage evolution of the MFE shown in Fig. 5. The dominating role of T-T annihilation in the triplet exciton decay has been suggested for EPH LEDs operating at large current densities.[11] In such a case one would expect the MFE to increase monotonically with magnetic field, reflecting the monotonous decrease of the $\gamma_{TT}(B)$ rate constant. Instead, the $\Delta\varphi_{EL}(B)/\varphi_{EL}(0)$ curves for Ir(ppy)$_3$- and PtOEP-doped EPH LEDs reveal a maximum at about 0.5 T that is not expected on the ground of the FSM theory.[25–27] But even if one considers the high magnetic field decrease in the MFE to be uncertain, due to a few points in this field range, and assumes a saturation trend to be more appropriate, the saturation onset at a similar B seems to contradict an order of magnitude difference in the triplet zero field splitting for Ir(ppy)$_3$ and PtOEP molecules, as pointed out in the above description of possible MFE phenomena. Furthermore, the decreasing gra-

dient in the MFE vs B curve for the PtOEP LED from the very beginning is at variance with the predictions of the FSM theory.[25–27] If T-T quenching is only a small correction to the dominating monomolecular decay of triplet states, the MFE on φ_{EL} can be expressed by[36]

$$\Delta\varphi_{EL}(\mathrm{B})/\varphi_{EL} \cong [\Delta\gamma_{\mathrm{Tq}}(\mathrm{B})/\gamma_{\mathrm{Tq}}][1-\gamma_{\mathrm{Tq}}\tau_{\mathrm{T}}n(1-2G\gamma_{\mathrm{TT}}\tau_{\mathrm{T}}^2)] - [\Delta\gamma_{\mathrm{TT}}(\mathrm{B})/\gamma_{TT}]G\gamma_{\mathrm{TT}}\tau_{\mathrm{T}}^2, \quad (1)$$

where G is the generation term of the excited states related directly to the current density, j, and n is the concentration of charge. The positive values of the MFE observed over the entire B and U ranges used are consistent with the predictions of Eq. (1). The relative variation of $\Delta\gamma_{\mathrm{Tq}}(\mathrm{B})/\gamma_{\mathrm{Tq}}$ differs, in general, from that of $\Delta\gamma_{\mathrm{TT}}(\mathrm{B})/\gamma_{\mathrm{TT}}$. In pyrene crystals, $\Delta\gamma_{\mathrm{Tq}}(\mathrm{B})/\gamma_{\mathrm{Tq}}$ has been shown to be a much weaker function of the applied magnetic field than that for $\Delta\gamma_{\mathrm{TT}}(\mathrm{B})/\gamma_{\mathrm{TT}}$,[36] though both decrease as the magnetic field increases. Assuming a similar relation holds for the present phosphor molecules, one would expect the overall effect to decrease as the magnetic field increases within the entire range of B used. Instead, a decreasing tendency appears only at the highest fields, $\mathrm{B}>0.5$ T. Finally, since no MFE on the driving current is observed for the phosphor-doped LEDs, the triplet enhancement of the electrode injection ability can be neglected, and the voltage increasing charge density ($n \cong \varepsilon_0\varepsilon\mathrm{U}/\mathrm{ed}^2$ under space-charge-limited conditions; see, e.g., Ref. 5) leads to an increasing number of triplet annihilation events on the carriers ($\mathrm{T}\text{-}\mathrm{D}_{\pm 1/2}$) and, consequently, to a reduction in the average triplet lifetime. As a result, the MFE should show up as a monotonically decreasing function of the applied voltage whenever $G(\mathrm{U})=\mathrm{const}$, the case suitable for photoenhanced currents.[36] However, in the EPH, the G term increases with applied voltage much stronger than the linear increase of n ($G=j/\mathrm{ed}\cong\varepsilon_0\varepsilon\mu\mathrm{U}^2/\mathrm{ed}^4$ for the space-charge-limited currents), and a voltage increase of the MFE is expected over the entire range of magnetic fields, the prediction at variance with experiment, where the field variation of φ_{EL} at lower magnetic fields is, within the experimental accuracy, voltage independent (Fig. 5). This reasoning concerns the TPD excited triplets as well, if formed by $e-h$ recombination on TPD molecules in the (phosphor:TPD:PC) emitter layer. By this argument we support the previous suggestion[3] that the excitation of phosphor molecules by energy transfer from triplets of TPD is of minor importance, and this is the recombination of electrons located on phosphor molecules with mobile holes that dominates the phosphor excited triplet formation.

In view of the above discussion, class (I) phenomena, though it cannot be excluded completely, seem at least insufficient to interpret the observed MFEs, the second and third class of the phenomena should be considered as a likely alternative since in all the cases emission originates from the *e–h* recombination possibly involving long-living $e\cdots h$ pair states as their precursors. A range of exchange energy values $|2J|$ must be invoked in order to explain the differences in the magnetic field strength dependence of the MFE for the LEDs studied, apparent in Fig. 4. Let us first consider the phosphor-doped LEDs. The general scheme of energy levels

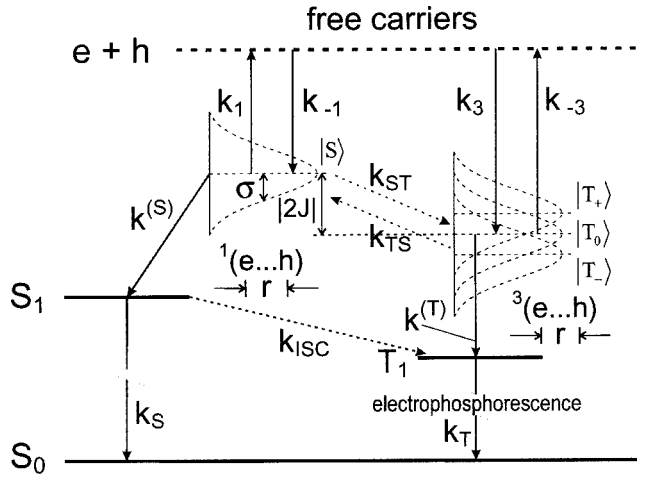

FIG. 6. The proposed energy-level diagram (not to scale) and electronic transitions leading to phosphorescent molecular triplet states (T_1). For explanation see the text.

and formation of excited molecular triplets (T_1) is provided in Fig. 6. Figure 6 also implies the existence of overlapping Gaussian energy bands of the $(e\cdots h)$ pairs due to static and dynamic disorder in noncrystalline organic solids.[37] The MFE measured on a macroscopic ensemble of molecules like organic solid films is an average over a large number of charge pairs, each of them characterized by a well-defined intercarrier distance and intermolecular orientation, which, however, are different for different charge pairs due to the random nature of the bimolecular recombination process, and the diagonal and off-diagonal disorder of solid samples. In random media, intermolecular distances and, consequently, the gas-to-solid shift energy of an excited state dipole and polarization energy of a carrier fluctuate. These fluctuations lead to the exciton and carrier energy bands to decompose into a Gaussian distribution in energy (E), $g(E)=(2\pi\sigma)^{-1/2}\exp(-E^2/2\sigma^2)$, typically $\sigma_{\mathrm{ex}}\cong 60$ meV and $\sigma_{\mathrm{pol}}\cong 0.1$ eV wide, respectively.[37] The latter imposes a similar broadening of the CP energy levels. There are two possible pathways for the formation of phosphorescent molecular triplets from free charge carriers ($e+h$): (i) the singlet state pathway (singlet route), where the singlet pair state $^1(e\cdots h)$ evolves into the excited molecular singlet, S_1, which can intersystem cross (k_{ISC}) into the triplet T_1, and (ii) the triplet state pathway (triplet route), where the triplet pair state $^3(e\cdots h)$ undergoes a radiationless transition $[k^{(\mathrm{T})}]$ to the molecular triplet T_1. Of two limiting cases, the strong ($k_{-1}\gg k^{(\mathrm{S})}+k_{\mathrm{ST}}; k_{-3}\gg k^{(\mathrm{T})}+k_{\mathrm{TS}}$)- and weak ($k_{-1}\ll k^{(\mathrm{S})}+k_{\mathrm{ST}}; k_{-3}\ll k^{(\mathrm{T})}+k_{\mathrm{TS}}$)-pair dissociation approximations, only the latter can lead to the magnetic field increase of the T_1 population and the positive MFE on EPH on the ground of type (IIB) phenomena. From the stationary kinetics for T_1 in the strong pair-dissociation limit, the EPH flux is proportional to the decay rate of triplet states, T_1, according to

$$\Phi_{\mathrm{EPH}}(\mathrm{B}) \propto k^{(\mathrm{S})}\epsilon_1^{-1} + [k^{(\mathrm{T})} + k_{\mathrm{TS}}k^{(\mathrm{S})}(k_1\epsilon_1)^{-1}] \times[\epsilon_3^{-1} + k_{\mathrm{ST}}(k_3\epsilon_1\epsilon_3)^{-1}] \times[1-k_{\mathrm{ST}}k_{\mathrm{TS}}(k_1k_3\epsilon_1\epsilon_3)^{-1}]^{-1}, \quad (2)$$

where $\epsilon_1 = k_{-1}/k_1$ and $\epsilon_3 = k_{-3}/k_3$ are the branching ratios in the formation of the pair states from free carriers. The magnetic field decreasing rate constants, $k_{ST}(B)$ and $k_{TS}(B)$, characteristic of class (IIB) phenomena, lead to a magnetic field decrease in $\Phi_{EPH}(B)$.

In contrast, the stationary kinetics in the weak-dissociation approximation case for the "singlet route" yields

$$\Phi_{EPH}(B) \propto k_1(1+\xi_S)^{-1} + [1+\xi_T(1+\xi_S)^{-1}] \times [k_3(1+\xi_T)^{-1}k_1\xi_S(1+\xi_S)^{-1} + (1+\xi_T)^{-1}] \times [1-\xi_S\xi_T(1+\xi_S)^{-1}(1+\xi_T)^{-1}]^{-1}, \quad (3)$$

with $\xi_S = k_{ST}(B)/k^{(S)}$ and $\xi_T = k_{TS}(B)/k^{(T)}$ standing for the branching ratios in the mixing of singlet, $|S\rangle$, and triplet, $|T_+\rangle$, $|T_0\rangle$, $|T_-\rangle$, states, which increases with the magnetic field following a magnetic field decrease in the rate constants $k_{ST}(B)$ and $k_{TS}(B)$ expected for type (IIB) phenomena. It is important to note that even in this approximation Φ_{EPH} is a decreasing function of B for the "triplet route." The resonance type curves in Figs. 4(b) and 4(c) with apparent maxima are principally predicted by class (III) phenomena due to the increasing $|S\rangle$-$|T_+\rangle$ mixing as the gradual increase of B shifts $|T_+\rangle$ towards the energy position of state $|S\rangle$, the maxima occur at $B_c = B_{max}$ corresponding approximately to the pair singlet-triplet splitting energy $|2J|$. We note that a similar result is obtained due to the $|S\rangle - |T_-\rangle$ mixing for the system with a negative $|S\rangle$-$|T_0\rangle$ energy gap. The gradual increase in B shifts then the $|T_-\rangle$ state down to the $|S\rangle$ state level with a concomitant increase of the rate constants k_{ST} and k_{TS}. The observed positive MFE results directly from Eq. (2), suggesting the strong-pair dissociation limit to be the adequate description. The shape of the curves is determined by the width of the pair state energy levels, and statistical distribution of the e–h separation distances, r. The B dependences of the MFE in Fig. 4 for both $Ir(ppy)_3$ and PtOEP phosphor-doped LEDs yield similar values of the most probable pair singlet-triplet splitting $|2J_{eff}| \cong g\beta B_{max} \cong 60\ \mu eV$ ($B_{max} \cong 0.5$ T). The r dependence of the exchange interaction is approximated by an exponential function $J(r) = J_0 \exp(-2r/L)$, where J_0 is the coupling matrix element for an electron donor-acceptor pair at van der Waals separation and L is a charge localization radius.[31] If, for example, one assumes $r = 0.85$ nm equivalent to the average distance between TPD and $Ir(ppy)_3$ molecules in the LED emitter from Fig. 4(b), and $L = 1.75$ Å as an average for these two molecules,[38] $J_0 \cong 4 \times 10^6$ mT follows with the experimental value of $J = J_{eff} \cong 260$ mT given above. The strongly r-dependent J reflects in the highly sensitive MFE (B) response to the intercarrier distance. It is enough to change r by 15% ($r = 1$ nm) to shift the resonance field to typically $B_{max} \cong 40$ mT. The weak-gradient increase in the low-field part of the MFE (B) curve for $Ir(ppy)_3$ LED, compared with that for the PtOEP LED, indicates an increased role of the exchange interaction, thus, a shorter intercarrier distance $\langle r \rangle$. This would suggest the mean distance between hole hopping molecular centers of TPD and electron-hopping molecular sites of the $Ir(ppy)_3$ to be shorter than that for the TPD-PtOEP system, the difference likely due to the steric constraints posed by the planar geometry of the larger PtOEP molecule. The observed difference in the magnitude of the MFE for $Ir(ppy)_3$ and PtOEP emitter-based LEDs can have diverse reasons. The most obvious is a difference in the effective hyperfine coupling constants due to different nuclear environments for electrons. A support for the resonance-type MFE observed for the phosphor-doped structures [Figs. 4(b) and 4(c)] comes from the voltage evolution of the MFE shown in Fig. 5. The reason is most probably due to the voltage-imposed reduction of the CP lifetime that is the increasing branching ratios ϵ_1 and ϵ_3. The applied voltage affects the MFE through the relation between ϵ_3^{-1} and $k_{ST}(k_3\epsilon_1\epsilon_3)^{-1}$ in the second term of Eq. (2). The voltage modulation of low magnetic field changes of $k_{ST}(B)$ is not practically seen when $\epsilon_3^{-1} \ll k_{ST}(B)(k_3\epsilon_1\epsilon_3)^{-1}$ equivalent to $k_{-1} \ll (k_1/k_3)k_{ST}(B)$, the resonance increase of $k_{ST}(B)$ at increasing magnetic fields and electric field increasing $k_{-1}(U)$ make this inequality less restrictive and a voltage increase of the MFE may be expected, which is indeed the case. Finally, a contribution of class (I) phenomena might be taken into consideration in the case of $Ir(ppy)_3$, where $T_1 \rightarrow$ TPD triplet transfer[38] increases the long-living triplet population on TPD that experiences quenching by a doublet species of the injected charge. The magnetic field reduction of the overall triplet-doublet interaction constant facilitates the back-transfer to emissive triplets of $Ir(ppy)_3$. This would explain a generally stronger MFE signal for EPH from the $Ir(ppy)_3$-based LED, but its decreasing trend at high magnetic fields contradicts theoretical predictions, and makes two former reasons more probable.

The electric field-independent MFE on the emission from the (TPD:PC)/PBD structure [Fig. 4(a)] reveals a monotonic increase with B up to above 0.5 T as observed previously with intramolecular exciplexes of pyrene and dimethylaniline systems.[29] It is underlain by the HFM of the formation of bimolecular excited states and a general analysis of its mechanism similar to that for the HFM on exciplex formation[31–34] applies, type (IIA) and (IIC) phenomena included. One could conjecture that the MFE in the phosphor-doped structures are a consequence of the MFE on the interface-formed ($TDP^+ \cdots PBD^-$) pairs, the final exciplex and electroplex products transferring energy to phosphor molecules. Such a mechanism is, however, unlikely since the B and U behavior in these two cases are completely different, as discussed above. A separate study of the MFE in a (TPD:PC)/PBD structure completed with other electron donor-electron acceptor LED systems is underway. In any case, the present results prove the effect of weak magnetic fields on optical emission, observed in the past with typical organic molecules, to be a universal phenomenon including heavy atom organometallic complexes. It is underlain by the fact that class II and III phenomena are related to intermolecularly separated charge carrier pairs, and the effect of intramolecular heavy atoms brings about the modification of the spin multiplicity of the excited states and magnitude of the hyperfine coupling. Class I phenomena are due to bimolecular reactions as well and the molecular structure (e.g., the presence of heavy atoms) can influence the magnitude of the magnetic field effect parameters rather than their physical meaning.

IV. CONCLUSIONS

We have observed the magnetic field increase of the electrophosphorescence from bilayer organic LEDs based on a metal-organic phosphor-doped blend of TPD and PC as the emitting and hole-transporting layers. Qualitative and quantitative differences are noted concerning the magnitude of the effect and its magnetic field dependence for the undoped (TPD:PC)/PBD system, and $Ir(ppy)_3$ and PtOEP phophor-doped (TPD:PC) emitter LED structures. The results have been discussed in terms of the fine structure modulation (FSM) of triplet exciton interactions and hyperfine modulation (HFM) of the formation of triplet states from the correlated electron-hole pairs. The self-consistent picture of the observed effects could be obtained only from the HFM-underlain phenomena in the strong pair-dissociation limit in which the triplets arise in the bimolecular electron-hole recombination process followed by a radiationless transition from triplet correlated charge pairs, taking into account the statistical distribution of the intercarrier distance in correlated electron-hole pairs preceding molecular excited states. The MFE on the low-efficiency emission from the phosphor undoped (TPD:PC)/PBD structure falls in the same general description scheme, though the exact kinetics and energy diagram of the excited species would differ, due to the different spin multiplicity and bimolecular nature of its emissive states, the effect that deserves further studies.

[1] M. A. Baldo, D. F. O'Brien, Y. You, A. Shoustikov, S. Sibley, M. E. Thompson, and S. R. Forrest, Nature (London) **395**, 151 (1998).

[2] C. Adachi, M. A. Baldo, M. E. Thompson, and S. R. Forrest, J. Appl. Phys. **90**, 5048 (2001).

[3] J. Kalinowski, W. Stampor, J. Mężyk, M. Cocchi, D. Virgili, V. Fattori, and P. Di Marco, Phys. Rev. B **66**, 235321 (2002).

[4] J. Kalinowski, J. Phys. D **32**, R179 (1999).

[5] J. Kalinowski, in *Organic Electroluminescent Materials and Devices*, edited by S. Miyata and H. S. Nalwa (Gordon & Breach, Amsterdam, 1997), Chap. 1.

[6] A. Köhler, J. S. Wilson, and R. H. Friend, Adv. Mater. (Weinheim, Ger.) **14**, 701 (2002).

[7] M. Wohlgenannt, K. Tandon, S. Mazumdar, S. Ramasesha, and Z. V. Vardeny, Nature (London) **409**, 494 (2001).

[8] M. Wohlgenannt and Z. V. Vardeny, J. Phys.: Condens. Matter **15**, R83 (2003).

[9] Y. Cao, I. D. Parker, G. Yu, C. Zhang, and A. Heeger, Nature (London) **397**, 414 (1999).

[10] J. Kim, P. K. H. Ho, N. G. Greenham, and R. H. Friend, J. Appl. Phys. **88**, 1073 (2000).

[11] M. A. Baldo, C. Adachi, and S. R. Forrest, Phys. Rev. B **62**, 10 967 (2000).

[12] J. Kalinowski, G. Giro, M. Cocchi, V. Fattori, and R. Zamboni, Chem. Phys. **277**, 387 (2002).

[13] J. Kalinowski, G. Giro, M. Cocchi, V. Fattori, and P. Di Marco, Appl. Phys. Lett. **76**, 2352 (2000).

[14] X. Jiang, S. Liu, M. S. Liu, P. Herguth, A. K.-Y. Jen, H. Fong, and M. Sarikaya, Adv. Funct. Mater. **12**, 745 (2002).

[15] O. Inganäs, as in Ref. 8, Chap. 3.

[16] J. Kalinowski, M. Cocchi, P. Di Marco, W. Stampor, G. Giro, and V. Fattori, J. Phys. D **33**, 2379 (2000).

[17] C. E. Swenberg and N. E. Geacintov, in *Organic Molecular Photophysics*, edited by J. B. Birks (Wiley, London, 1973), Vol. 1, Chap. 10.

[18] N. E. Geacintov and C. E. Swenberg, in *Organic Molecular Photophysics*, edited by J. B. Birks (Wiley, London, 1975), Vol. 2, Chap. 8.

[19] K. Okamoto, N. Oda, A. Itaya, and S. Kusabayashi, Chem. Phys. Lett. **35**, 483 (1975).

[20] E. L. Frankevich, A. A. Lymarev, I. Sokolik, F. E. Karasz, S. Blumstengel, R. H. Baughman, and H. H. Hörhold, Phys. Rev. B **46**, 9320 (1992).

[21] F. Ito, T. Ikoma, K. Akiyama, Y. Kobori, and S. Tero-Kubata, J. Am. Chem. Soc. **125**, 4722 (2003).

[22] J. Kalinowski, J. Szmytkowski, and W. Stampor, Chem. Phys. Lett. **378**, 380 (2003).

[23] H. Hayashi and S. Nagakura, Bull. Chem. Soc. Jpn. **51**, 2862 (1978).

[24] Y. Sakaguchi, H. Hayashi, and S. Nagakura, Bull. Chem. Soc. Jpn. **53**, 39 (1980).

[25] R. C. Johnson and R. E. Merrifield, Phys. Rev. B **1**, 896 (1970).

[26] P. Avakian, R. P. Groff, R. E. Kellog, R. E. Merrifield, and A. Suna, in *Organic Scintillators and Liquid Scintillation Counting*, edited by D. L. Horrocs and C. T. Peng (Academic, New York, 1971), p. 499.

[27] K. Lendi, P. Gerber, and H. Labhart, Chem. Phys. **20**, 145 (1977).

[28] A. Carrington and A. D. McLachlan, *Introduction to Magnetic Resonance with Applications to Chemistry and Chemical Physics* (Harper & Row, New York, 1967).

[29] R. De, Y. Fujiwara, T. Haino, and Y. Tanimoto, Chem. Phys. Lett. **315**, 383 (1999).

[30] H. Cao, K. Miyata, T. Tamura, Y. Fujiwara, A. Katsuki, C. H. Tung, and Y. Tanimoto, J. Phys. Chem. A **101**, 407 (1997).

[31] H. Staerk, H.-G. Busmann, W. Kühnle, and R. Treichel, J. Phys. Chem. **95**, 1906 (1991).

[32] F. Ito, T. Ikoma, K. Akiyama, Y. Kobori, and S. Tero-Kubota, J. Am. Chem. Soc. **125**, 4772 (2003).

[33] E. A. Weiss, M. A. Ratner, and M. R. Wasielewski, J. Phys. Chem. **107**, 3639 (2003).

[34] A. S. Lukas, P. J. Bushard, E. A. Weiss, and M. R. Wasielewski, J. Am. Chem. Soc. **125**, 3921 (2003).

[35] A. Weller, in *The Exciplex*, edited by M. Gordon and W. R. Ware (Academic, New York, 1975), p. 23.

[36] H. Bouchriha, M. Schott, and J. L. Fave, J. Phys. (France) **36**, 399 (1975).

[37] H. Baessler, Phys. Status Solidi B **107**, 9 (1981).

[38] J. Kalinowski, W. Stampor, M. Cocchi, D. Virgili, V. Fattori, and P. Di Marco, Chem. Phys. **297**, 39 (2004).